

Intrinsic mirror birefringence measurements for the Any Light Particle Search (ALPS)

Claire Baum

University of Florida

August 11, 2016

Abstract

In this paper, I use a heterodyne polarimeter to measure the intrinsic birefringence of a mirror at different orientations and examine how its birefringence is affected in an applied magnetic field. These measurements will assist the vacuum magnetic birefringence measurement in the Any Light Particle Search (ALPS) experiment. For a mirror at 45° incidence, 0° incidence, and 0° incidence with an applied magnetic field, the relative effective path length difference between two 1064 nm laser beams was ≈ 26.6 nm, 4.871 ± 0.046 nm, and 16.58 ± 0.11 nm respectively.

1. INTRODUCTION

The Any Light Particle Search (ALPS) experiment is a search for Weakly Interacting Sub-eV Particles (WISPs) at the Deutsches Elektronen-Synchrotron (DESY) in Hamburg, Germany. These WISPs are new particles predicted by extensions of the Standard Model that may explain natural phenomena such as dark matter and provide evidence supporting variations of string theory [1].

The ALPS experiment consists of the ALPS I and ALPS II experiments. ALPS II consists of ALPS IIa, ALPS IIb, and ALPS IIc. ALPS I marked the beginning of the ALPS experiment and ran from 2007 until 2010 [2], [3]. ALPS II is the continuation of ALPS I and first runs for ALPS II are projected to occur in late 2016 [4]. Like ALPS I, ALPS IIc is a light shining through a wall (LSW) experiment. A general schematic of the ALPS IIc LSW experiment is shown in Figure 1. LSW experiments consist of two cavities permeated by a magnetic field on either side of a wall. Photons are shone into the first cavity, oscillate into WISPs that traverse the wall, then oscillate back into photons in the second cavity. Thus, ALPS researchers can study WISPs by detecting photons that seemingly pass through the wall.

The setup of ALPS II also allows researchers to measure the vacuum birefringence in a magnetic field. Birefringence is a property in which materials have a refractive index dependent on the polarization and propagation direction of incident light. This vacuum magnetic birefringence is predicted by QED and has yet to be confirmed experimentally [5]!

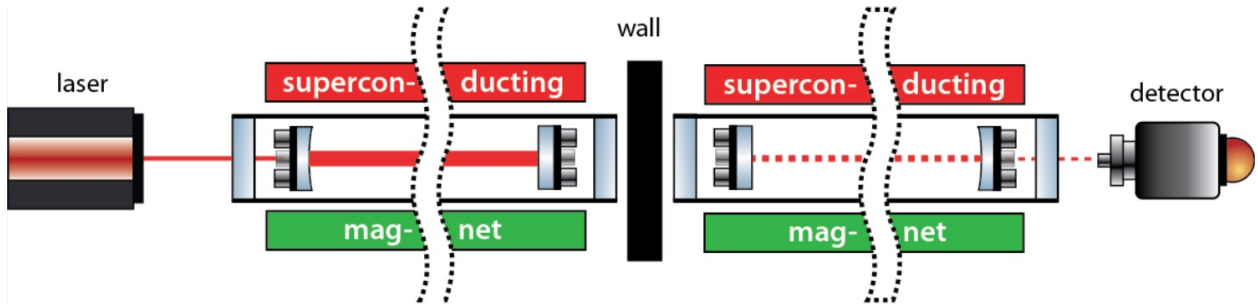


Figure 1: The ALPS II experiment is a LSW experiment. Infrared laser photons are shone into a cavity and oscillate into WISPs that can pass through nontransparent matter (in this case, a wall). These WISPs then oscillate back into photons in a cavity on the other side of the wall. Thus, it appears as if light has shone through a wall! Image credit goes to <https://alps.desy.de/e191931/>.

In order to make a reliable vacuum magnetic birefringence measurement, the birefringence of the optics used in the ALPS experiment must be known. An apparatus called a heterodyne polarimeter can be used to measure the birefringence of such optical devices. In this paper, I use a heterodyne polarimeter to measure the intrinsic birefringence of a mirror at different orientations and examine how its birefringence is affected in an applied magnetic field. In addition, I report on the effectiveness of using a heterodyne polarimeter to measure the birefringence of optical components. These measurements will assist ALPS researchers in determining how optical components will affect the vacuum birefringence measurement and how to best measure their birefringence.

2. METHODS

A. The heterodyne polarimeter

A schematic of the heterodyne polarimeter used to measure intrinsic mirror birefringence is shown in Figure 2. This apparatus was used to measure the relative phase difference between two orthogonally polarized laser beams incident on a birefringent source (BF source). The greater the relative phase shift, the greater the birefringence of the birefringent source. The heterodyne polarimeter consisted of two 1064 nm lasers, a BF source, two photodetectors (PDs), and an assortment of optical components.

The two lasers (L1 and L2) were locked at a frequency of choice within the accepted frequency range of the experiment's electronics. The frequency at which the lasers are locked is the frequency difference, or beat frequency, between the two lasers. Thus, the frequency difference between the two lasers remained fixed even though the individual laser frequencies drifted. Faraday isolators were mounted in front of either laser to prevent unwanted back reflections into the lasers.

Half wave plates (HWPs) were placed in front of either laser's isolator for power control purposes. These HWPs were used to adjust the power output of the large polarizing beam splitter (PolBS) at the center of the setup. Light that is horizontally polarized, or p-polarized, is transmitted through polarizing beam splitters. Light that is vertically polarized, or s-polarized, is reflected by polarizing beam splitters. Rotating a HWP either increases the amount of p-polarized light and decreases the amount of

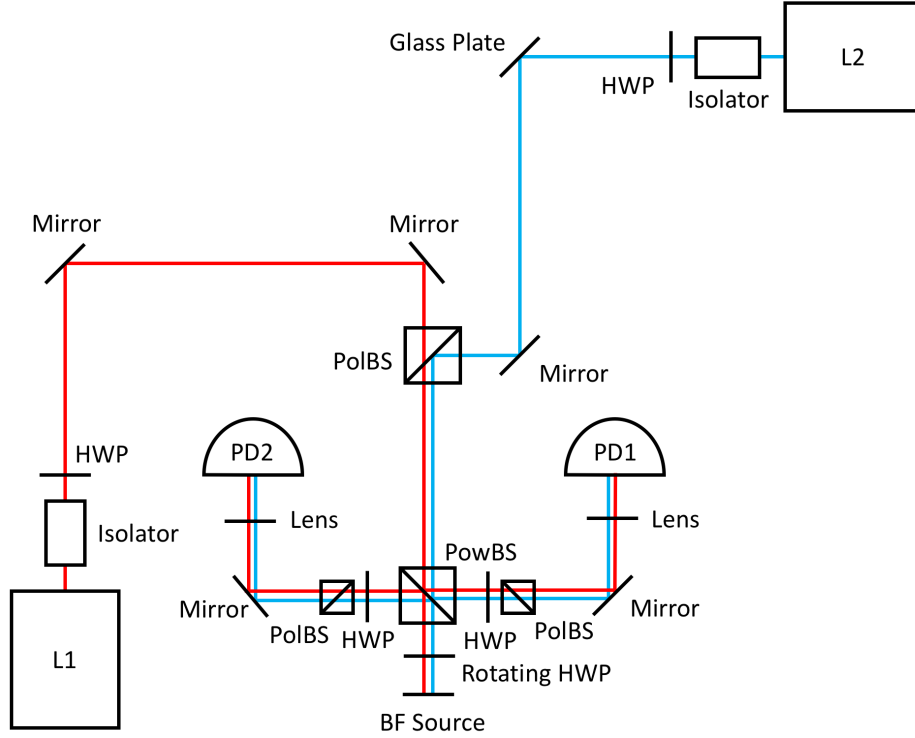


Figure 2: A schematic of the heterodyne polarimeter used to measure intrinsic mirror birefringence is shown above. Two overlapping and orthogonally polarized laser beams are incident on a birefringent source (BF source). As birefringent materials cause a polarization-dependent phase shift in incident light, the incident laser beams acquire a phase difference relative to each other. The amplitude of this phase shift depends on the orientation of the laser beams' orthogonal polarization. For example, two laser beams that are horizontally and vertically polarized respectively may undergo a larger relative phase difference than laser beams polarized at 45° and -45° relative to the horizontal axis respectively. Thus, the amplitude of the relative phase difference should oscillate if the orientation of the laser beams' orthogonal polarization is rotated at some frequency. This orientation rotation is accomplished by a rotating half wave plate (rotating HWP) that rotates the laser beam orientation at four times the rotation frequency of the rotating HWP.

s-polarized light or vice versa. Thus, the HWP was rotated to control the amount of light that was transmitted through and reflected by the polarizing beam splitter.

Two mirrors were placed after the HWP for L1 whereas a glass plate and a mirror were placed after the HWP for L2. Although both lasers were the same model (Innolight Mephisto OEM NE), L2 output over 100 mW more than L1. Thus, a glass plate was used to make the L1 and L2 beam powers more comparable by the time both beams overlapped at the first polarizing beam splitter. The mirrors and glass plate were also used in steering the laser beams such that the beams were overlapping after the first polarizing beam splitter.

The first polarizing beam splitter was used to overlap the laser beams from L1 and L2. It was also used to isolate the p-polarization of the L1 one beam and the s-polarization of the L2 beam such that the beams were orthogonally polarized upon entering the power beam splitter (PowBS). The overlapping and orthogonally polarized laser beams then entered a 50:50 power beam splitter after the first polarizing beam splitter. Half of the overlapping light was reflected toward the optics leading to PD1. The other half of the overlapping light was transmitted toward the optics leading to the BF source.

The light that was reflected toward the optics leading to PD1 first passed through a HWP and polarizing beam splitter. The HWP rotated the polarization of the overlapping laser beams and the polarizing beam splitter isolated the horizontally polarized component of both beams such that both beams contributed about the same amount of power upon exiting the polarizing beam splitter. The isolation of this horizontally

polarized component is necessary as the beat frequency is maximized when the two laser beams are overlapping and in the same polarization. The photodetectors were not able to detect the high frequencies of the individual lasers, but they were able to detect the fixed beat frequency. After the HWP and polarizing beam splitter, the beams then reflected off of a mirror, passed through a lens, and entered photodetector PD1. The mirror was used to help steer the laser beams into PD1 and the lens was used to converge the beams onto the small active area of PD1. Photodetector PD1 was placed near the focus of the lens and was used in locking lasers L1 and L2. Furthermore, the signal entering PD1 was used as a reference for the signal entering PD2.

The light that was transmitted toward the optics leading to the BF source first passed through rotating HWP controlled by a brushless motor. This rotating HWP rotated the orientation of the laser beams' orthogonal polarizations at four times the rotation frequency of the HWP. The rotating, orthogonal beams then reflected off of a BF source and acquired a relative phase difference cause by the birefringence of the BF source. In this experiment, the BF source included New Focus 5104 mirrors at 45° and 90° relative to the incoming laser beams (i.e. 45° and 0° angles of incidence respectively). Additionally, birefringence measurements were performed on a mirror at 0° incidence with a permanent magnet (U.S. Patent #5,528,415) placed immediately in front of the mirror; the magnitude of the magnetic field was about 4.5 kG at the mirror's surface. The light reflected by the BF source then passed through the rotating HWP once more, returning to the same polarization it had when it entered the rotating HWP. Half of this light was then transmitted through the power beam splitter. The other half was reflected by the power

beam splitter and entered the same optics setup as that between the power beam splitter and PD1. The power incident on the photodetectors ranged from about 0.5 to 3 mW.

The beat frequency entering PD2 should have a phase difference relative to the beat frequency entering PD1 since the light entering PD2 reflected off of the BF source. As the rotating HWP rotated the light incident on the BF source at four times the rotation frequency of the HWP, this relative phase difference should oscillate at four times the rotation frequency of the HWP as well.

B. Laser locking

The laser locking electronics are depicted in Figure 3. As the heterodyne polarimeter does not necessarily operate in the same way for different beat frequencies, the lasers were locked to prevent drift in the beat signal between the two lasers. Additionally, the lasers were locked to avoid non-linear effects, allowing for the best possible common mode noise rejection.

Photodetector PD1 was used to lock lasers L1 and L2. The output from PD1 was split into three signals. The first signal was viewed on a spectrum analyzer to determine the strength of the beat signal and assist in locking. The second signal was mixed with a function generator signal at the desired locking frequency. Thus, the mixer output a signal containing two frequencies: the sum of the PD1 and function generator frequencies and the difference between the PD1 and function generator frequencies. The third signal was sent to the Moku:Lab phasemeter for data collection.

The mixed PD1 and function generator signals were then sent through a low-pass filter to remove the higher frequency component of the mixed signal. The remaining low frequency component of this mixed signal was then sent into a phase-locked loop box (PLL box). This PLL box consisted of analog components and was created at the University of Florida. The PLL box output two variable voltages that controlled the frequency of L1 based on the PLL box input signal. If the input signal was zero frequency (DC), then the beat frequency between the two lasers was the same as the function generator frequency. Thus, the beat frequency was at the desired frequency as set by the function generator and the L1 laser frequency did not need adjustment. If the input signal was at a non-zero frequency (AC), then the beat frequency between the two lasers was not the same as the function generator frequency. Thus, the beat frequency was not at the desired frequency and the PLL box output two voltages to adjust the L1 laser frequency.

The PLL box had a "fast" and "slow" voltage output. The "slow" output was sent to the laser temperature control input in the back of the laser control box to adjust L1's temperature, and thus frequency, over long periods of time. The "fast" output was split into two signals. The first signal was viewed on an oscilloscope to assist in locking. The second signal was sent directly to laser L1 to control the piezo crystal inside the laser, thus controlling L1's frequency over short periods of time.

The 10 MHz reference signal for the spectrum analyzer and Moku:Lab was provided by the function generator. Further specifications of components are listed in Table 1.

Table 1: Component specifications

Component	Frequency	Impedance
TDS 2024 Oscilloscope	200 MHz	1 M Ω
HP 8591E Spectrum Analyzer	9 kHz - 1.8 GHz	50 Ω
Textronic AFG3251 Function Generator	240 MHz	50 Ω
EOT ET-3000A Photodetector	2 GHz maximum	-
Mini-Circuits BLP-21.4 Low Pass Filter	DC - 22 MHz	50 Ω
Mini-Circuits ZAD-3H+ Mixer	0.05 - 200 MHz	-
Mini-Circuits ZFSC-3-1-S+ Power Splitter	1 - 500 MHz	50 Ω

C. Data collection and analysis

The data collection electronics are also shown in Figure 3. Data from PD1 and PD2 were collected using the Moku:Lab. The Moku:Lab hardware is shown in Figure 4. The signals from PD1 and PD2 were sent to the two inputs of the Moku:Lab. The phases of these two signals were tracked using the Moku:Lab phasemeter as shown in Figure 5. This phase data was collected at 120 S/s, saved as a CSV file, then analyzed in MATLAB.

The frequency and phase differences between the PD1 and PD2 signals were taken in MATLAB and plotted over time. The birefringence signal should appear as an oscillation in the phase difference data at four times the rotation frequency of the rotating HWP in Figure 2. This HWP was mounted in the Thorlabs Compact Direct Drive

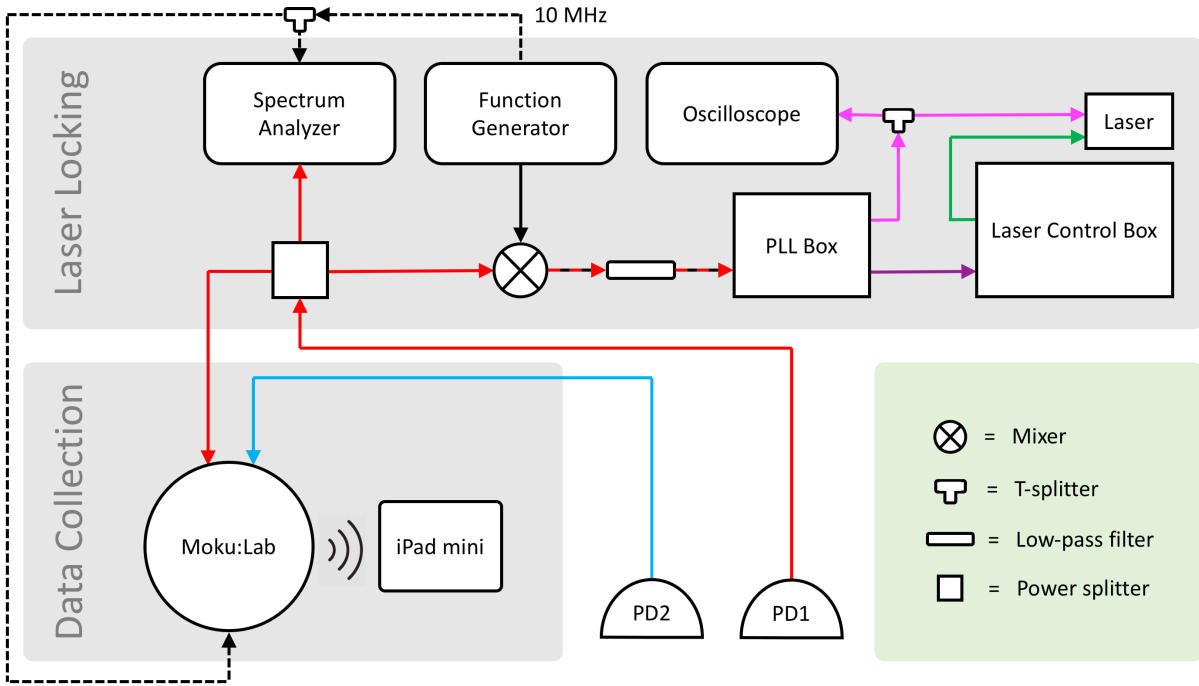


Figure 3: A schematic of the laser locking and data collection electronics is shown above. The signal from PD1 was sent through a phase-locked loop to control the frequency of laser L1 and keep the beat frequency constant. The signals from both PD1 and PD2 were sent to the Moku:Lab. The Moku:Lab application on an iPad mini contained a phasemeter interface for data collection.

Rotation Mount (DDR05) controlled by the Thorlabs K-Cube Brushless DC Servo Controller (KBD101). The servo controller was controlled by the Thorlabs APT System Software on a computer. Rotation sequences were specified on the APT System Software for the various data collection runs.

The fast Fourier transform (FFT), power spectral density (PSD), and demodulation of the phase difference data were also calculated using MATLAB for the longer data runs. The FFT displayed the relative magnitudes of the frequencies present in

the phase difference data. The PSD displayed the noise density in cycles per square root of hertz over the frequencies present in the phase difference data. The demodulation process entailed multiplying the phase difference signal by a MATLAB-generated sine and cosine signal at a frequency of four times the rotation frequency of the rotating HWP. Sums over each cycle of the multiplied signals were then plotted versus cycle number. Demodulation at the correct frequency would result in two bunches of data points on the plot. One bunch of data points would be representative of the sine wave demodulation and be distributed about a constant value. The other bunch of data points would be representative of the cosine wave demodulation and be distributed about a different constant value. The phase of the MATLAB-generated sine and cosine signals was then adjusted such that one of the bunches of data points was distributed about zero. This distribution indicates that the phase and frequency of the MATLAB-generated signals have been correctly matched to that of the original phase difference signal. The phase difference amplitude is extracted from the phase difference data by taking the mean of each cycle in the run, taking the mean of the the cycle means, then multiplying by two. This factor of two arises from trigonometric identities; multiplying a sine or cosine signal by itself results in an AC term at twice the original sine or cosine frequency and a DC term at the original signal amplitude divided by two.



Figure 4: Above is an image of the Moku:Lab hardware and the corresponding Moku:Lab application on the iPad mini. The Moku:Lab's consisted of two signal inputs and one, 10 MHz external reference input. The Moku:Lab application included an oscilloscope, spectrum analyzer, phase meter, waveform generator, data logger, and soon-to-be lock-in amplifier. This application was linked to the Moku:Lab hardware via wifi. Image credit goes to <http://www.liquidinstruments.com>.

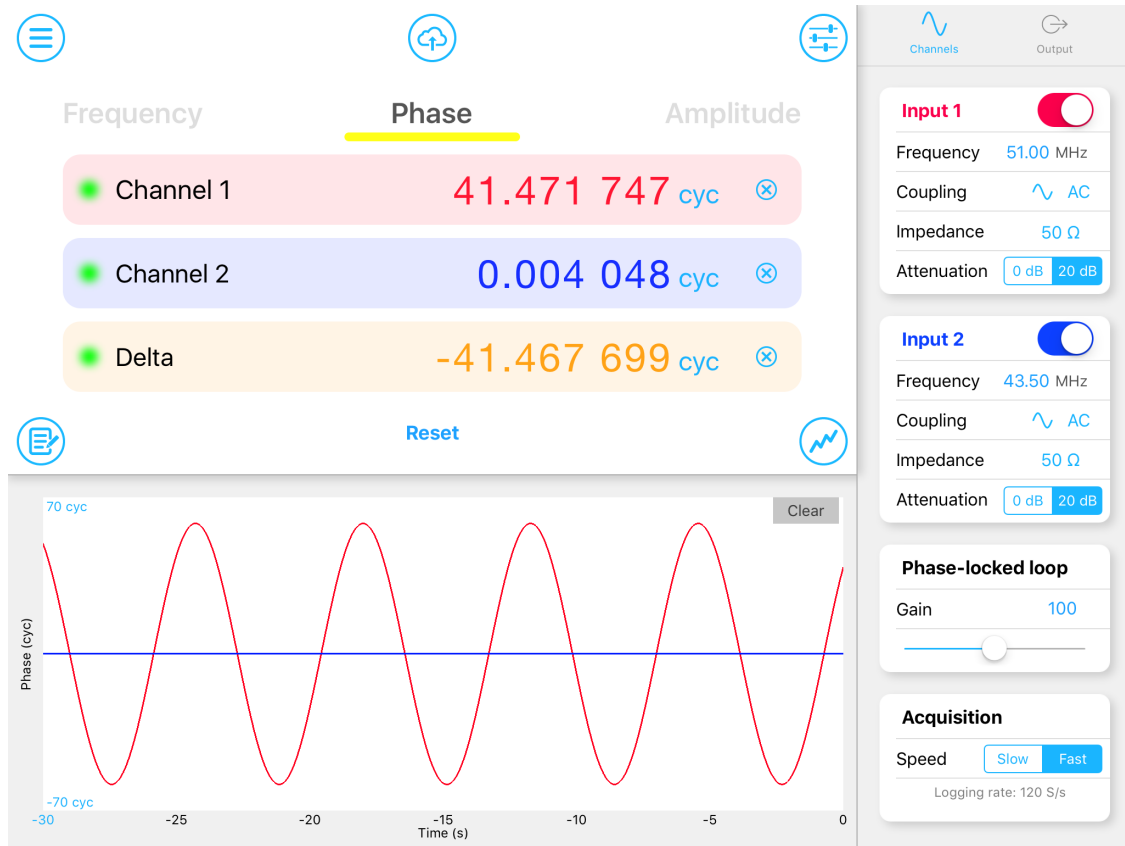


Figure 5: Above is a screenshot of the phasemeter interface in the Moku:Lab application on the iPad mini. Readouts of the frequency, phase, and amplitude of the input signals in channels 1 and 2 were displayed in the upper left panel. In the screenshot above, only the phase readout is displayed. In the sidebar on the right of the screenshot, input and data acquisition parameters can be specified. The user must manually enter the frequency to be tracked by the phasemeter in this sidebar. Data was acquired in the Moku:Lab phasemeter on the "fast" (120 S/s) setting then saved as a binary or CSV file which can be saved to an SD card in the Moku:Lab hardware, emailed, saved to the cloud, or uploaded to Dropbox. Furthermore, the impedance was set to 1 M Ω and the attenuation was set to 0 dB.

3. RESULTS

A. Birefringence of a mirror at 45° incidence

Figures 6 and 7 display the birefringent measurements of a mirror at 45° incidence over 15 seconds. The laser light reflected off of a mirror at 45°, reflected off of another mirror at 0° incidence, then reflected off of the 45° incidence mirror once more. The PD1 beat signal was about 444 mVpp and the PD2 beat signal was about 270 mVpp as read on an oscilloscope. The lasers were locked at 55.2 MHz. These birefringence measurements of a mirror at 45° incidence were preliminary tests of the heterodyne polarimeter before moving on to birefringence measurements of a mirror at 0° incidence.

The amplitude of the phase difference signal between the PD1 and PD2 signals in Figure 7 is about 0.05 cycles. This phase difference is the relative phase difference between the two laser beams. As the laser beams reflected off of the 45° incidence mirror twice, one reflection off of the 45° incidence mirror should yield a relative phase difference amplitude of 0.025 cycles (approximating a zero phase difference amplitude from the 0° incidence mirror). This phase difference amplitude corresponds to a relative effective path length difference of ≈ 26.6 nm (0.025 cycles multiplied by 1064 nm).

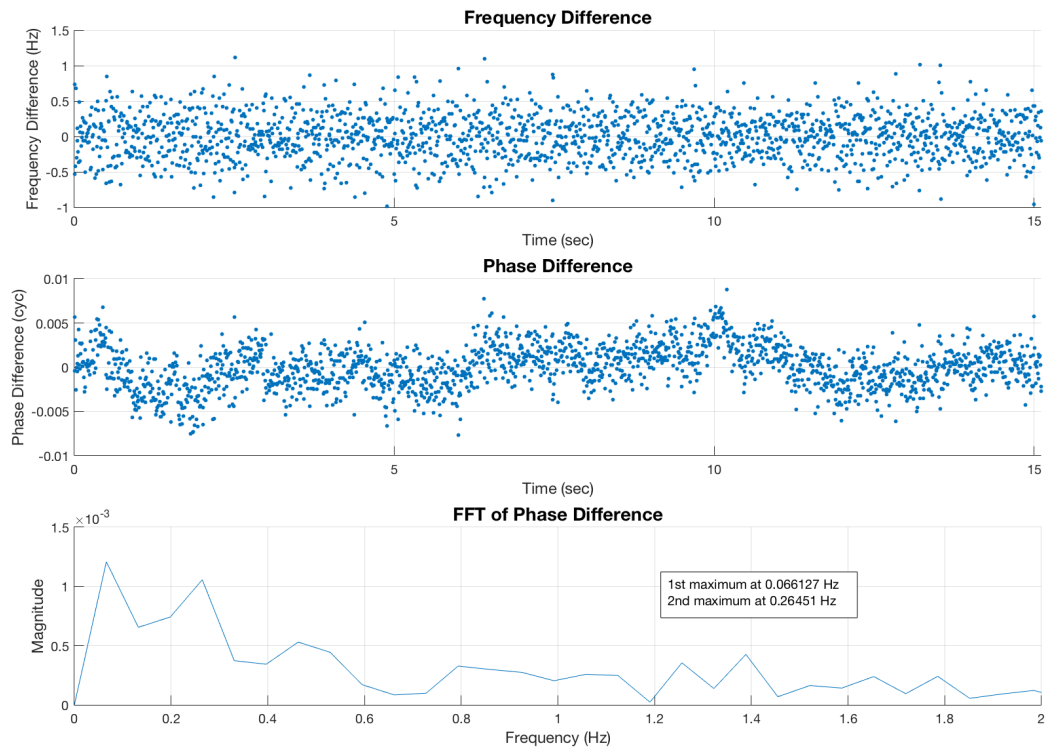


Figure 6: The plots above display birefringence measurements of a mirror at 45° incidence for no rotation of the rotating HWP. As expected, the birefringence signal at four times the rotation frequency of the HWP is not present.

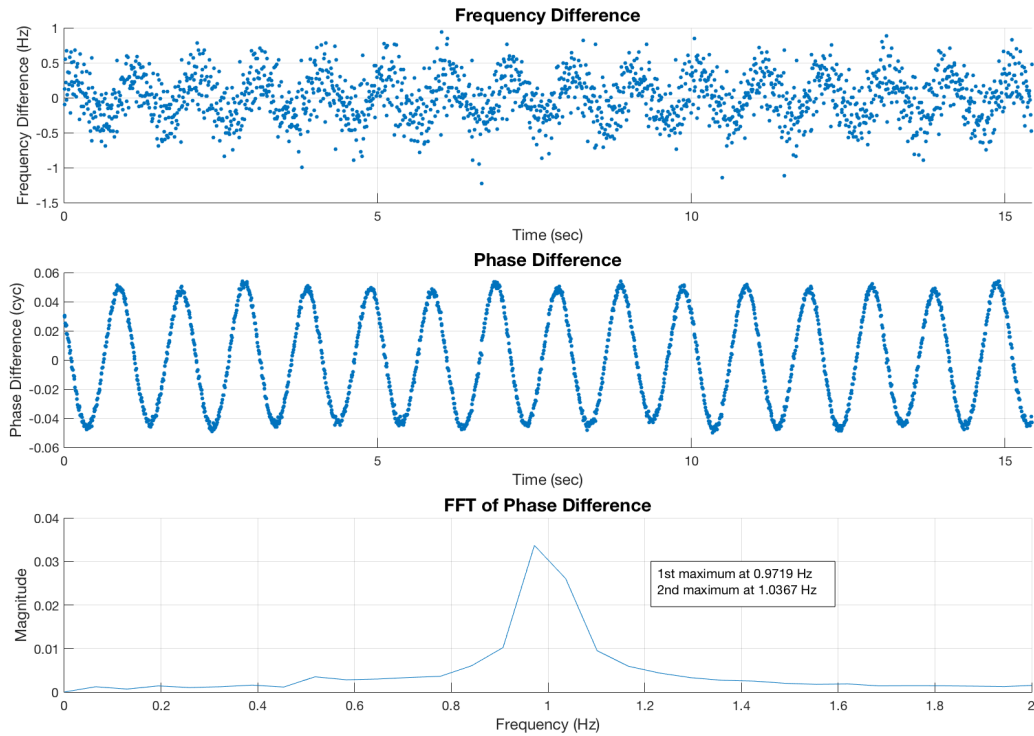


Figure 7: The plots above display birefringence measurements of a mirror at 45° incidence for a HWP rotation frequency of 90 deg/sec (0.25 Hz). As shown by the FFT, the birefringence signal appears at 1 Hz (four times the rotation frequency of the HWP). The frequency difference oscillates at the same frequency as the phase difference oscillation because the frequency is the time derivative of the phase. Note that the peaks in the phase difference oscillation correspond to the zero-crossings in the frequency difference oscillation.

B. Birefringence of a mirror at 0° incidence

Figures 8, 9, 10, 11, and 12 display the birefringent measurements of a mirror at 0° incidence over 10 minutes at a HWP rotation frequency of 90 deg/sec (0.25 Hz). The PD1 beat signal was about 346 mVpp and the PD2 beat signal was about 346 mVpp as read on an oscilloscope. The lasers were locked at 55.2 MHz.

Using the demodulation method as described in the Methods section, the amplitude of the phase difference signal between the PD1 and PD2 signals was $457.82 \times 10^{-5} \pm 4.34 \times 10^{-5}$ cycles. The error is taken as the standard deviation of the means of each multiplied signal cycle divided by the square root of the number of cycles. This phase difference amplitude corresponds to a relative effective path length difference of 4.871 ± 0.046 nm.

C. Birefringence of a mirror at 0° incidence in a magnetic field

Figures 13, 14, 15, 16, and 17 display the birefringent measurements of a mirror at 0° incidence over 10 minutes. The PD1 beat signal was about 300 mVpp and the PD2 beat signal was about 300 mVpp as read on an oscilloscope. The lasers were locked at 55.2 MHz.

Using the demodulation method as described in the Methods section, the amplitude of the phase difference signal between the PD1 and PD2 signals was $155.85 \times 10^{-4} \pm 1.04 \times 10^{-4}$ cycles. This phase difference amplitude corresponds to a relative effective path length difference of 16.58 ± 0.11 nm.

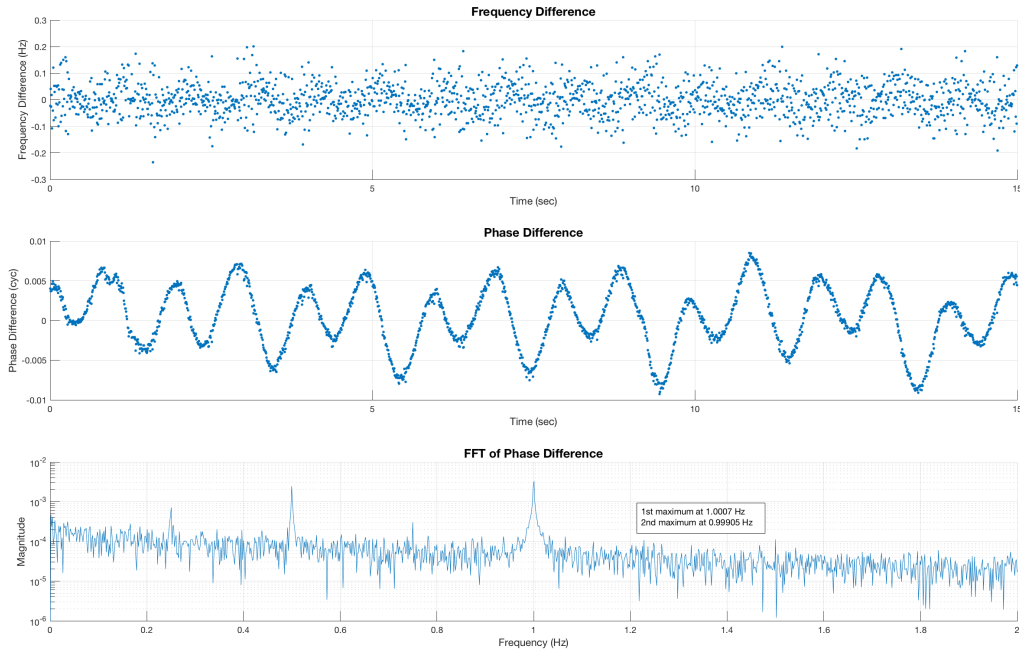


Figure 8: The plots above display birefringence measurements of a mirror at 0° incidence for a HWP rotation frequency of 90 deg/sec (0.25 Hz). As shown by the FFT, the birefringence signal appears at 1 Hz (four times the rotation frequency of the HWP). Additional frequency components at 0.25 Hz, 0.5 Hz, and 0.75 Hz. These frequency components may have been caused by back reflections from the rotating HWP, light passing through the HWP at non-zero incidence, and shifts in the HWP location as the rotating mount rotated.

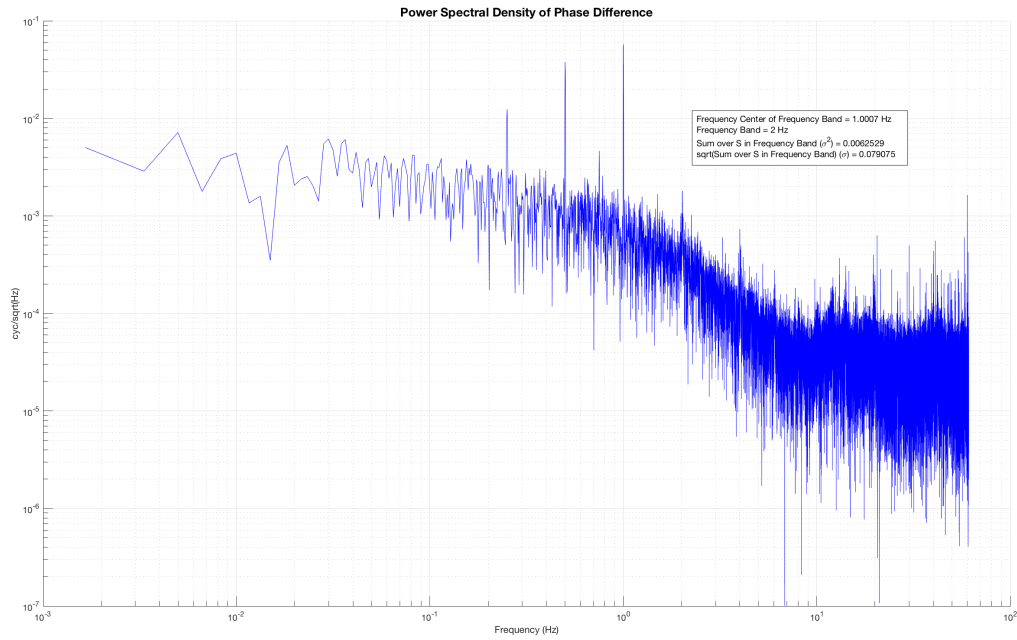


Figure 9: The plot above displays the power spectral density (PSD) of the phase difference data in Figure 8. Main peaks occur at 0.25 Hz, 0.5 Hz, and 0.75 Hz and 1 Hz. Note that the standard deviation should be and is within a factor of two of the standard deviations in Figures 11 and 12. As the noise level drops by about a factor of 10 between 1 and 10 Hz, the rotating HWP should be operated at higher frequencies (where the noise is lower).

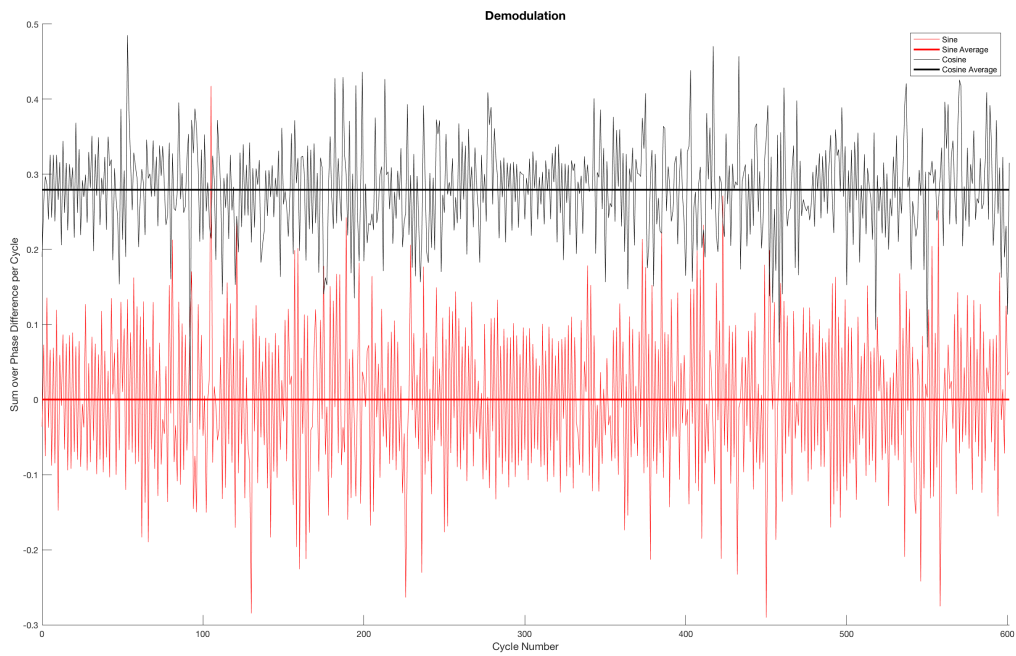


Figure 10: The plot above displays the demodulation of the phase difference signal in Figure 8 as described in the Methods section.

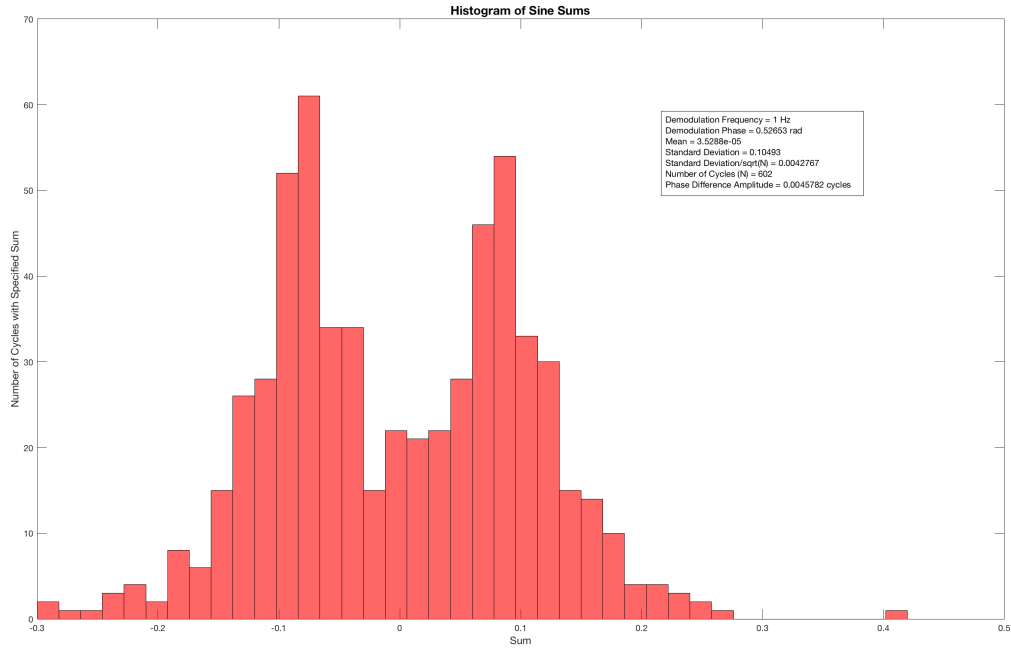


Figure 11: The plot above displays a histogram of the cycle sums for demodulation by a MATLAB-generated sine wave for the mirror at 0° incidence measurement. The non-Gaussian behavior is a result of demodulation at four times the rotation frequency of the rotating HWP. The frequencies at one, two, and three times the rotating frequency of the rotating HWP are not eliminated, but instead averaged out over time.

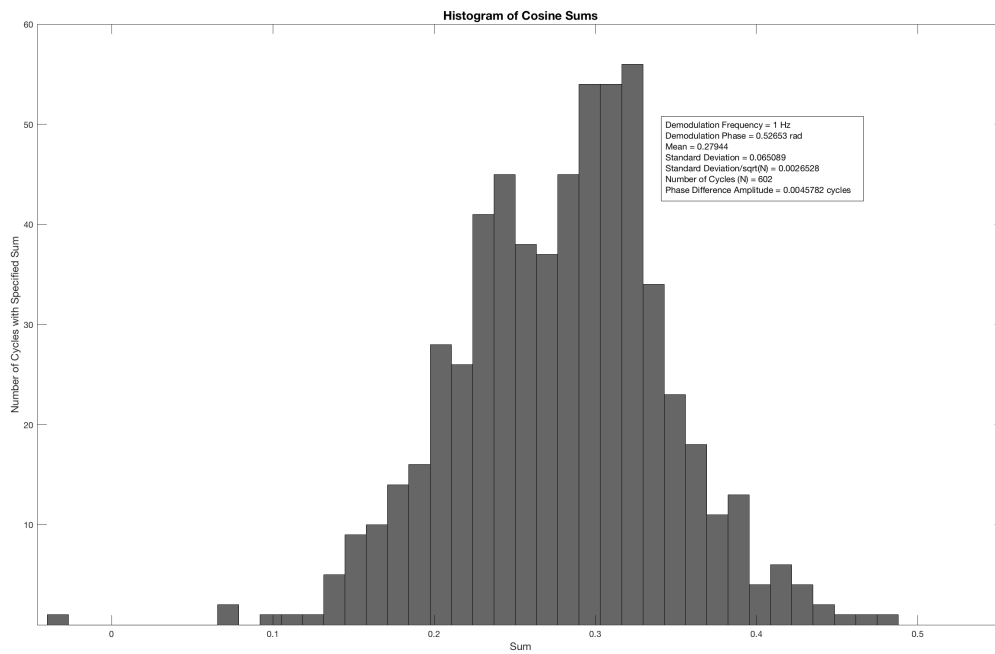


Figure 12: The plot above displays a histogram of the cycle sums for demodulation by a MATLAB-generated cosine wave for the mirror at 0° incidence measurement.

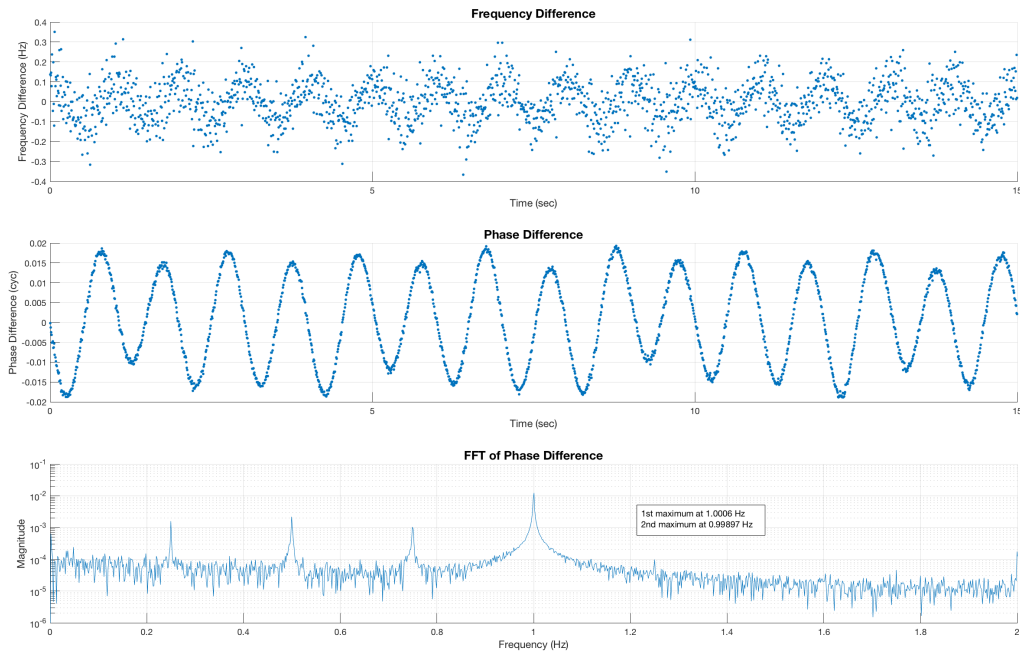


Figure 13: The plots above display birefringence measurements of a mirror at 0° incidence with an applied magnetic field for a HWP rotation frequency of 90 deg/sec (0.25 Hz). As shown by the FFT, the birefringence signal appears at 1 Hz (four times the rotation frequency of the HWP).

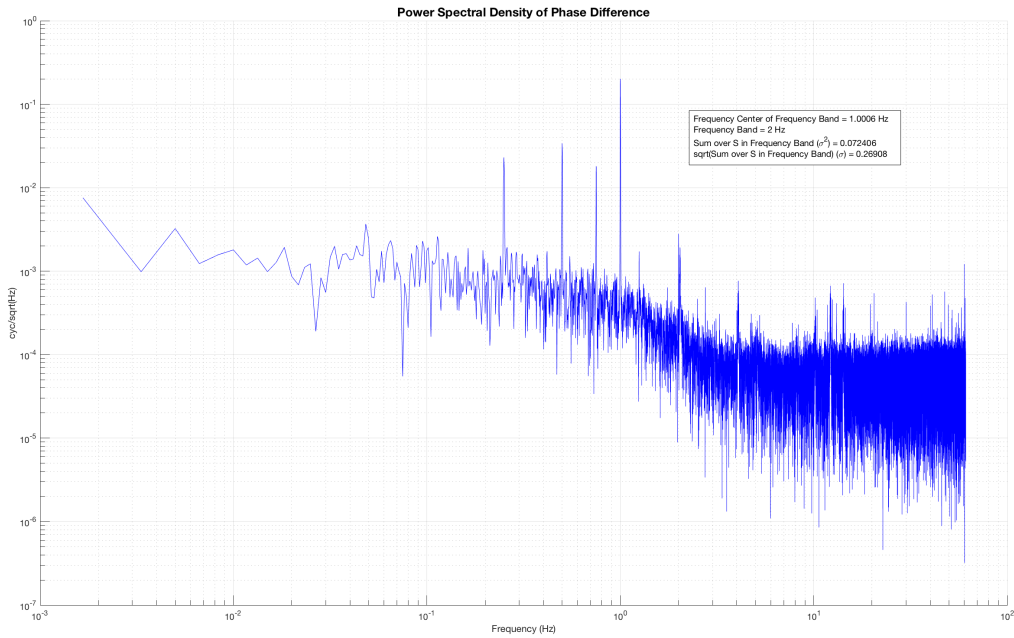


Figure 14: The plot above displays the power spectral density (PSD) of the phase difference data in Figure 13. Main peaks occur at 0.25 Hz, 0.5 Hz, and 0.75 Hz and 1 Hz. As the noise level drops by about a factor of 10 between 1 and 10 Hz, the rotating HWP should be operated at higher frequencies (where the noise is lower).

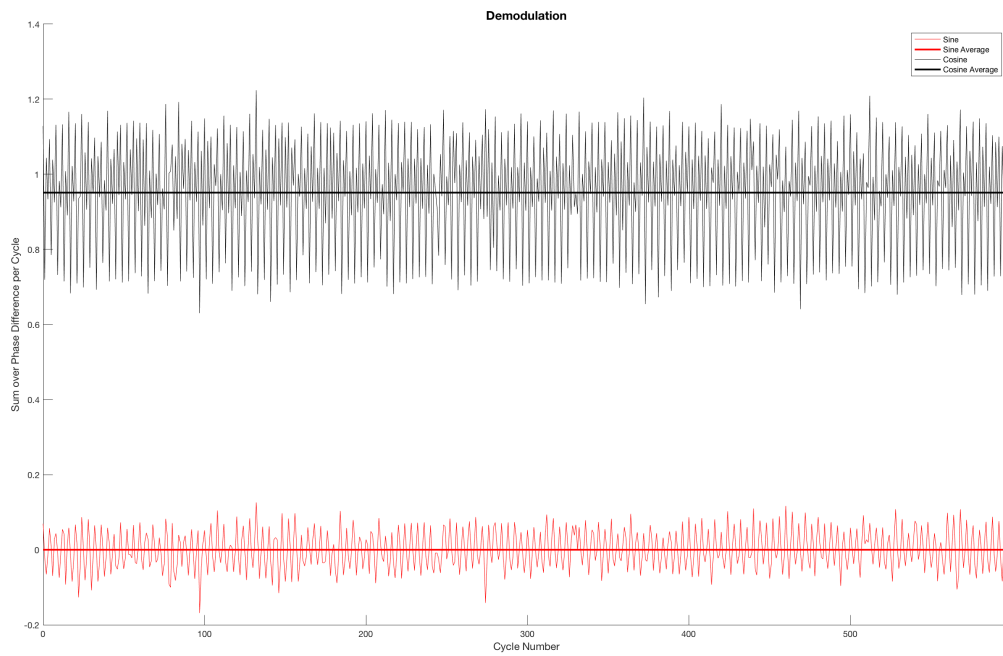


Figure 15: The plot above displays the demodulation of the phase difference signal in Figure 13 as described in the Methods section.

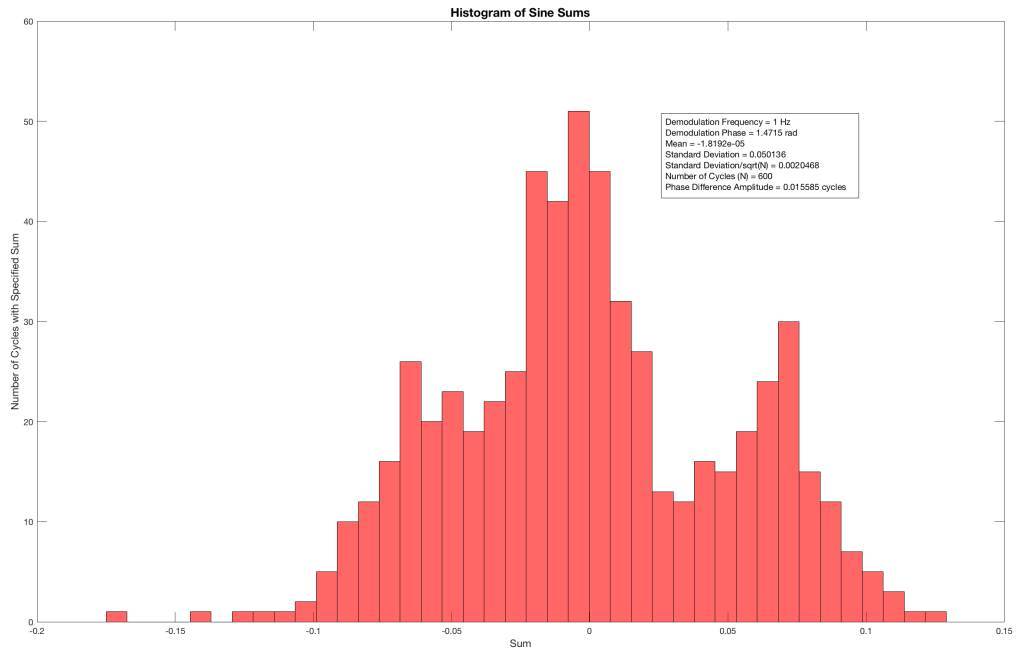


Figure 16: The plot above displays a histogram of the cycle sums for demodulation by a MATLAB-generated sine wave for the mirror at 0° incidence with an applied magnetic field measurement.

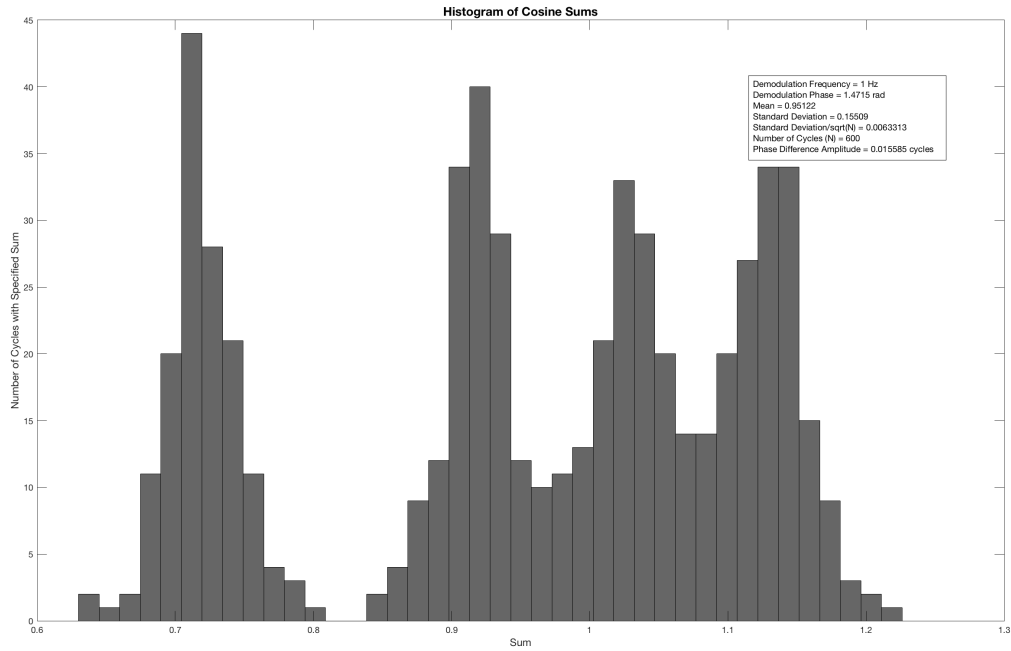


Figure 17: The plot above displays a histogram of the cycle sums for demodulation by a MATLAB-generated cosine wave for the mirror at 0° incidence with an applied magnetic field measurement. As in Figure 11, the non-Gaussian behavior is likely a result of demodulation at four times the rotation frequency of the rotating HWP.

4. CONCLUSION

Using a heterodyne polarimeter, birefringence measurements for a New Focus 5104 mirror were performed at 45° incidence, 0° incidence, and 0° incidence with an applied magnetic field. For a mirror at 45° incidence, 0° incidence, and 0° incidence with an applied magnetic field, the relative effective path length difference between two 1064 nm laser beams was ≈ 26.6 nm, 4.871 ± 0.046 nm, and 16.58 ± 0.11 nm respectively. To increase the sensitivity of the heterodyne polarimeter, runs should be taken at a higher HWP rotation frequency (in the lower noise region) and for longer periods of time.

These measurements are the first steps toward the vacuum magnetic birefringence measurement in the Any Light Particle Search (ALPS) experiment. The general birefringence effects of a standard 1064 nm mirror are now known. In the future, more stable mirrors will be necessary in ALPS. Using the heterodyne polarimeter presented in this report, further birefringence measurements for different mirrors can be made to help find the optimal mirrors for the ALPS experiment. Additionally, the presence of an applied magnetic field greatly increased the amplitude of the birefringent signal. This magnetic field-dependent birefringence must be analyzed in depth and taken into account when designing ALPS and selecting optical components. After improving birefringence measurement methods and selecting the optimal optical components for ALPS, the birefringence of all of the optical components in ALPS will be measured to determine how their birefringence will effect the vacuum magnetic birefringence measurement.

Potential improvements to the experiment presented in this report include digital

laser locking and tracking the polarization of the light incident on the BF source as the rotating HWP rotates. In addition, the length of data collection runs was greatly limited by how long the lasers remained locked; the frequency of laser L1 was not very stable and caused the lock to break many times. If possible, it might be a good consistency check to collect data using a different phasemeter as well. Future measurements might include a mirror at 0° incidence for different angles of incidence of the rotating HWP, a LIGO mirror at 0° incidence, measurements at a higher HWP rotation frequency, measurements at different locking frequencies, and more measurements including the perma magnet at different distances in front of the BF source. Additional records on this experiment can be located at www.phys.ufl.edu/darkcosmos/lab.

ACKNOWLEDGMENTS

I'd like to thank Professor Selman Hershfield and the University of Florida physics department for the fantastic experience I've had as a summer 2016 physics REU student. I'd also like to thank Professor Guido Mueller, Professor David Tanner, and my labmates in the LIGO, LISA, and ALPS collaborations at the University of Florida for the big help and delicious lunch outings! This work was funded by NSF grant DMR-1461019.

APPENDIX A

An image of the experiment has been provided in Figure 18 for reference. The power beam splitter is slightly rotated relative to 0° incidence to prevent back reflections from the light incident on the BF source from entering PD1.

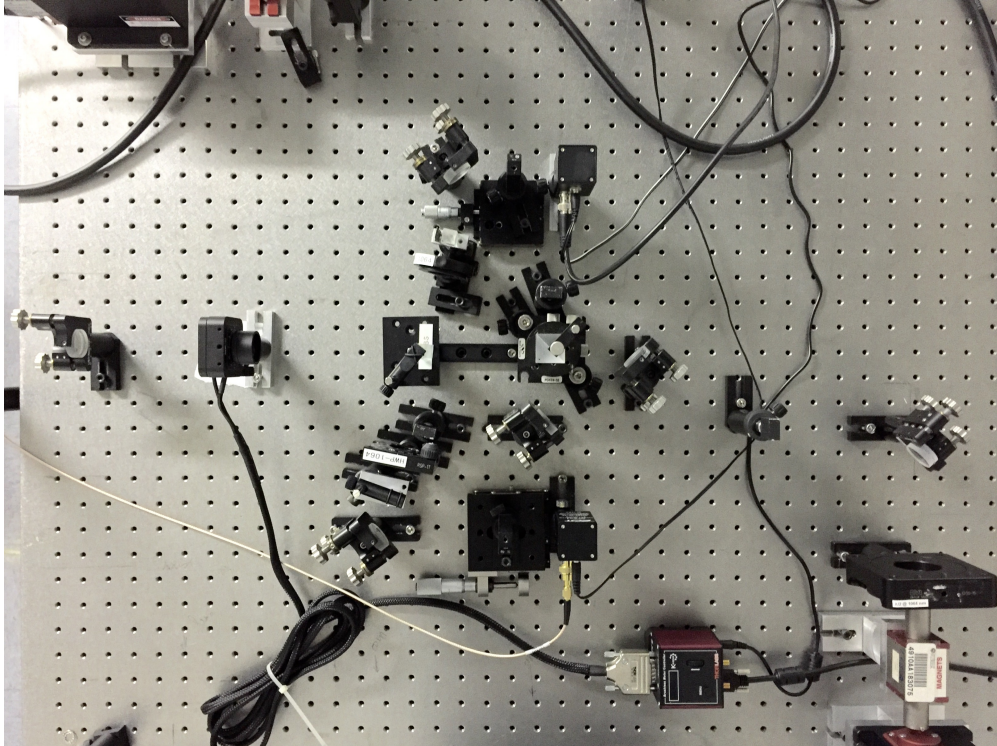


Figure 18: Above is an image of the experimental setup in the lab. Laser L1 is in the upper left corner and laser L2 is in the lower right corner.

APPENDIX B

The beam profiles and parameters of lasers L1 and L2 are displayed in Tables 2 and 3 and Figures 19 and 20 for reference. The beam profiles and parameters were obtained using a CCD camera and MATLAB. The w_0 and z_0 values in the beam parameter tables were calculated via MATLAB scripts and the divergence angle was calculated using $\theta = \frac{\lambda}{\pi w_0}$. The beam parameters of L1 and L2 were not matched in this experiment.

Table 2: Beam Parameters of laser "LOKI" (L1)

Beam Parameters: LOKI		
Parameter	Symbol	Value
Wavelength (nm)	λ	1064
Waist radius (μm)	w_0	188.945
Waist location (m)	z_0	-0.0584
Divergence angle (radians)	θ	0.00179

Table 3: Beam Parameters of laser "ODIN 2" (L2)

Beam Parameters: ODIN 2		
Parameter	Symbol	Value
Wavelength (nm)	λ	1064
Waist radius (μm)	w_0	122.873
Waist location (m)	z_0	-0.0832
Divergence angle (radians)	θ	0.00276

LOKI beam profile at 0.07 mW

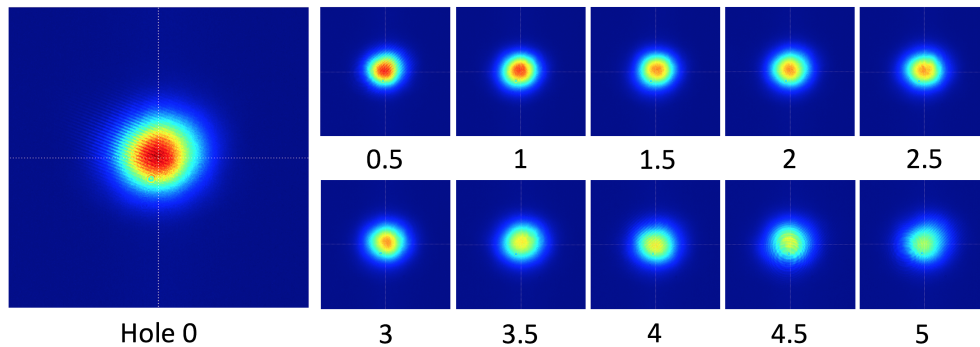


Figure 19: The image above displays the beam profile of L1 (labelled "LOKI" in the lab) at different distances away from the laser. The hole numbers correspond to the holes on the optics table where holes were one inch apart. Hole 0 corresponds to the CCD camera being 11.024 inches away from the laser base and the point at which the laser power was 0.07 mW. Thus, Hole 0.5 corresponds to the CCD camera being 11.525 inches away from the laser base, Hole 1 correspond to the CCD camera being 12.024 inches away from the laser base, and so on.

ODIN 2 beam profile at 0.17 mW

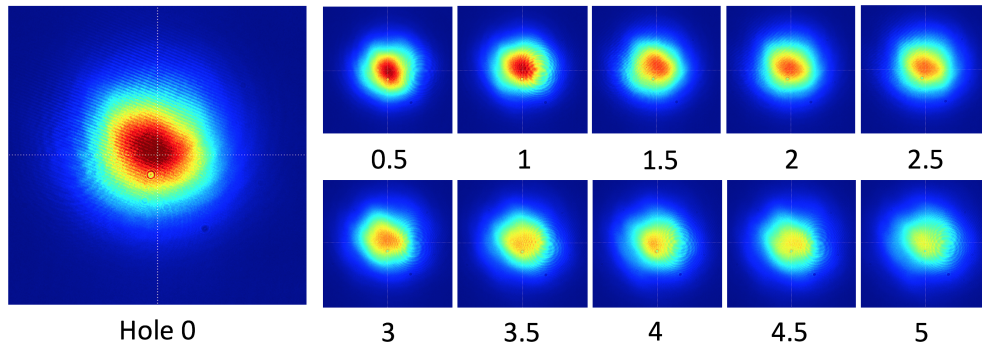


Figure 20: The image above displays the beam profile of L2 (labelled "ODIN 2" in the lab) at different distances away from the laser. The hole numbers correspond to the holes on the optics table where holes were one inch apart. Hole 0 corresponds to the CCD camera being 11.024 inches away from the laser base and the point at which the laser power was 0.17 mW. Thus, Hole 0.5 corresponds to the CCD camera being 11.525 inches away from the laser base, Hole 1 correspond to the CCD camera being 12.024 inches away from the laser base, and so on.

References

- [1] <https://alps.desy.de>
- [2] <https://alps.desy.de/e141063/>
- [3] A. Lindner *et al.* (ALPS Collaboration), "New ALPS results on hidden-sector lightweights." *Phys. Lett. B* **689** (4-5), 149-155 (2010).
doi:10.1016/j.physletb.2010.04.066.
- [4] <https://alps.desy.de/e191931/>
- [5] K. Ehret (ALPS Collaboration), "The ALPS Light Shining Through a Wall Experiment - WISP Search in the Laboratory." 2010, <http://arxiv.org/abs/1006.5741>.